

Supported Imidazolium functionalized POSS hybrids as Palladium Platform for C–C Cross Coupling Reactions

Carla Calabrese,^[a,b] Vincenzo Campisciano,^[a] Fabiana Siragusa,^[a] Leonarda F. Liotta,^[c] Carmela Aprile,^{*,[b]} Michelangelo Gruttadauria,^{*,[a]} and Francesco Giacalone^{*,[a]}

Department of Biological, Chemical and Pharmaceutical Sciences and Technologies, University of Palermo Viale delle Scienze, Ed. 17 90128, Palermo (Italy)

Istituto per lo Studio dei Materiali Nanostrutturati ISMN-CNR, Via Ugo La Malfa 153, 90146 Palermo (Italy)

Laboratory of Applied Materials Chemistry (CMA), University of Namur, 61 rue de Bruxelles, 5000 Namur (Belgium)

KEYWORDS heterogeneous catalysis, POSS, Palladium, C–C cross-coupling, imidazolium hybrids

ABSTRACT: Supported imidazolium modified polyhedral oligomeric silsesquioxanes (POSS) have been used as platform for Pd^{II} species. Such material was firstly characterized by means of TGA, solid state NMR, TEM, XPS, SAXS, porosimetry and ICO-OES and it was successfully tested as pre-catalyst in C–C cross couplings, namely Suzuki-Miyaura and Heck reactions. In both cases, the solid proved to be highly efficient and easily recoverable from the reaction mixture. The recyclability was verified for up to seven cycles without showing any activity decrease. Interestingly only Pd^{II} was detected in the reused catalyst in the Heck reaction. Therefore, the versatility of our material was extensively investigated by using various aryl halides endowed with electron-donating or electron-withdrawing groups. Our palladium nanocomposite was able to promote both Suzuki and Heck reactions down to 0.0007 mol% showing outstanding turnover frequency (TOF) values of 113,515 and 32,162, respectively. The excellent outcome of the reactions could be ascribed to the textural properties of the SBA-15 support and the presence of the imidazolium-POSS nanocage within the pores of SBA-15.

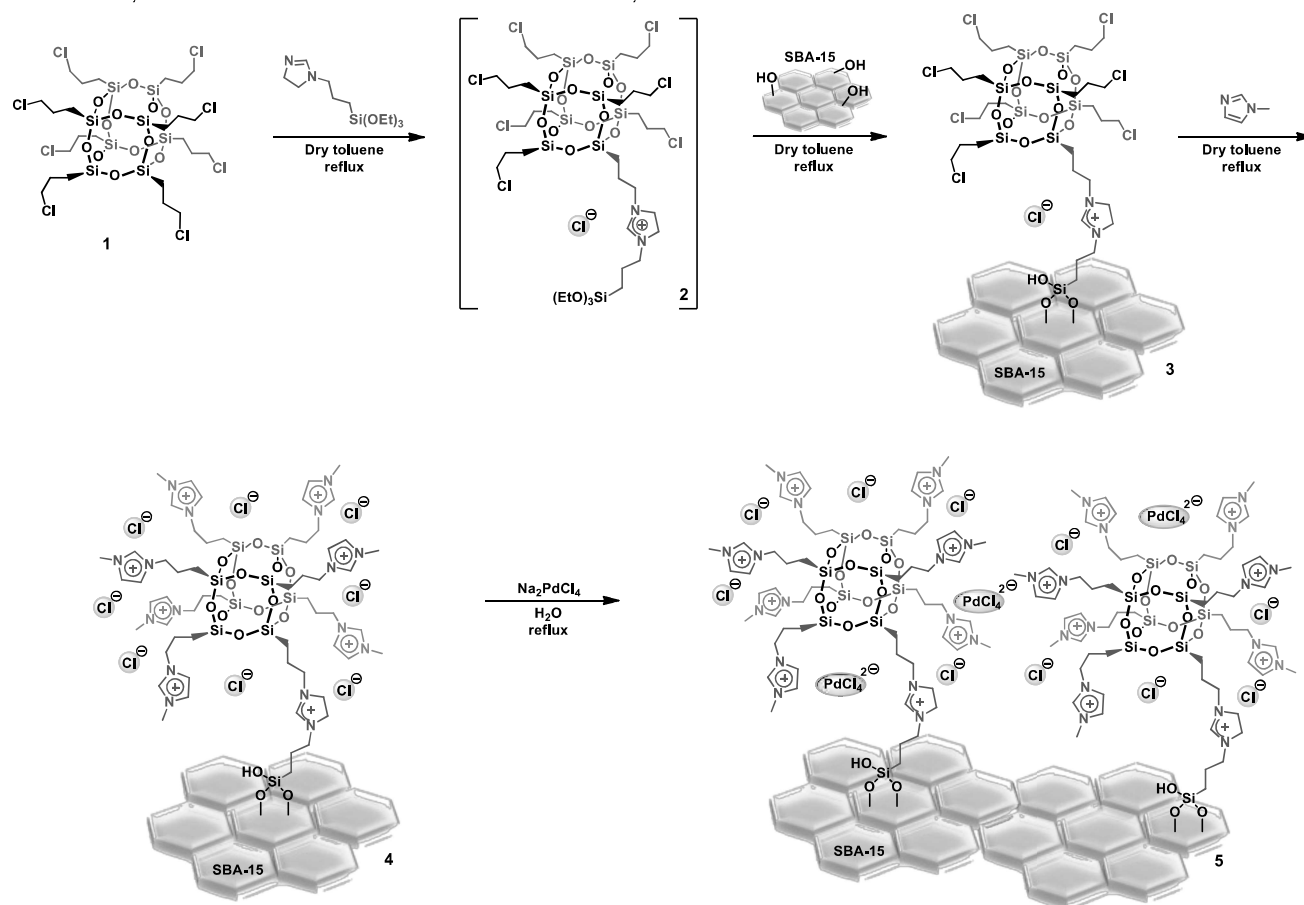
INTRODUCTION

The increasing demand of highly active and recyclable catalytic materials for C–C cross coupling reactions pushed the scientific research toward the design of performing heterogeneous hybrids. The importance of C–C bond formation process is well known in organic synthesis including the preparation of pharmaceuticals, drugs, agrochemicals, natural products, and the design of organic semiconductors. In particular, palladium catalyzed C–C cross coupling reactions emerged as one of the most versatile tools as testified not only by the awarding of the Nobel Prize in Chemistry in 2010 to R. F. Heck, E.-C. Negishi and A. Suzuki, but also by the continuous growing publications on this field.^{1,5} In order to improve the sustainability of such reactions, a broad variety of palladium based heterogeneous catalysts has been developed.^{6,8} In this context, the reduction of waste generation is indeed connected to an easy recovery and reuse of the catalyst itself. Furthermore, a lower metal contamination of the final products is typically achieved with heterogeneous catalyst by comparison to the corresponding homogeneous reaction conditions. On this last point, it is worth to look at the strict regulations on the maximum allowable amount of metal contaminants, for example, for pharmaceutical compounds (< 5 ppm).⁹ Palladium catalysts have been immobilized into a plethora of pre-functionalized solid supports such as mesostructured¹⁰ and amorphous silica,¹¹⁻¹² zeolites,¹³ organic polymers,^{14,15} ionic liquids,¹⁶ magnetic nanocomposites,¹⁷⁻¹⁸ carbon nanoforms,¹⁹⁻²³ halloysite nanotubes,^{24,25} and MOFs²⁶⁻²⁸. Moreover, supported imidazolium salts emerged as promising platform for both Pd nanoparticles (NPs)²⁹⁻³⁰ and Pd^{II} species.^{16, 31-34} In doing so, silica stands out from other solid supports because of its useful features, such as high surface area, good thermal and mechanical stability, widespread availability, and easy covalent functionalization strategies covering a broad range

of organic or organo-metallic moieties.^{11, 35-36} Recently, we reported a series of highly active catalytic materials based on palladium NPs supported on imidazolium-C₆₀ hybrids covalently grafted onto several supports, namely amorphous silica gel, mesostructured SBA-15 and silica coated maghemite.³⁷ The use of silica supports for the system Pd NPs@imidazolium salt@C₆₀, allowed to obtain heterogeneous nanocatalysts with excellent performances for C–C cross couplings. Polyhedral oligomeric silsesquioxanes (POSS), have been modified with imidazolium functionalities and used as support for Pd^{II}.³⁸⁻⁴⁰ Such hybrids were employed as pre-catalysts for Suzuki-Miyaura and Heck couplings. POSS nanostructures are a family of appealing organic-inorganic hybrid molecules composed of an inorganic siloxane nanocage surrounded by tailoring organic peripheries.⁴¹ POSS display high thermal and mechanical stability together with a wide tunability of functional side groups. Such interesting properties result in a broad range of applications involving POSS hybrids for the design of sensors, electronic devices, polymer nanocomposites, liquid crystals, biomaterials, solar cells and catalytic supports.⁴²⁻⁴⁷ In a recent work,⁴⁸ we reported the design, synthesis and application of a series of imidazolium functionalized POSS nanostructures covalently immobilized onto silica supports. Such materials were successfully used as heterogeneous catalysts for the conversion of carbon dioxide into cyclic carbonates. Herein, we propose imidazolium modified POSS hybrids grafted onto mesostructured SBA-15 as solid supports for the immobilization of Pd^{II} species. Furthermore, inspired by the promising catalytic performance of POSS imidazolium tetrachloropalladate salts,³⁸ we designed a novel heterogeneous hybrid following a modular synthesis in which POSS units were previously grafted into the solid support in order to be modified with imidazolium chloride moieties. The solid was treated with Na₂PdCl₄ to give the final hybrid by ionic ex-

change. Next, our material was successfully tested as pre-catalyst in Suzuki-Miyaura and Heck reactions.

Scheme 1. Synthesis of Pd^{II} imidazolium functionalized POSS hybrid.



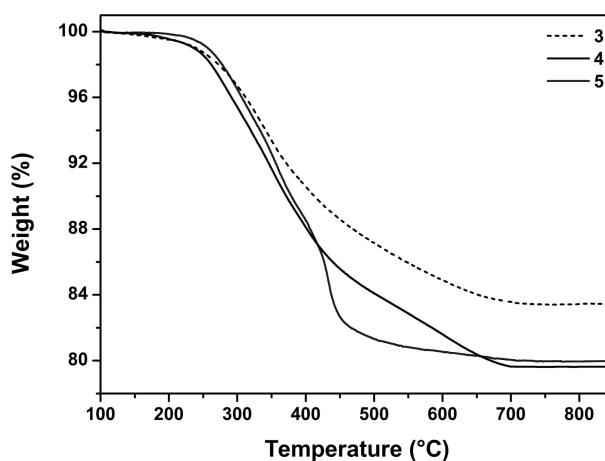
RESULTS AND DISCUSSION

According to a literature procedure,⁴⁸ octakis(3-chloropropyl)octasilsesquioxane (compound 1) was reacted with triethoxy-3-(2-imidazolyl)propylsilane to give compound 2 that was directly grafted onto mesostructured SBA-15 to afford the solid 3. The functionalization of supported POSS nanostructures with imidazolium chloride peripheries (material 4) was obtained from the reaction between material 3 and 1-methylimidazole. The imidazolium loading of solid 4 was estimated by means of combustion chemical analysis (C, H, N) and was found to be 0.81 mmol/g.

This synthetic strategy allowed to obtain a promising catalytic support endowed with a specific surface area of 272 m²/g, total pore volume of 0.87 cm³/g, and pore size distribution around 14 nm. The interesting textural properties of the solid make this material suitable for high flow catalytic applications. Considering its high value of pore size distribution, enabling internal diffusion paths, the hybrid 4 was designed as a sort of nano-reactor based on imidazolium modified POSS units as solid support for Pd species.

For doing so, the solid 4 was treated with a solution of Na₂PdCl₄ to give the final material 5 by anionic metathesis reaction. The thermal behavior of the final hybrid 5 and its precursor 3 and 4 was investigated by means of thermogravimetric

analysis (TGA, Figure 1). The decomposition of organic functionalities started in the range 240-250 °C, being the solid 5



slightly more stable than its precursor 3 and 4. The good thermal robustness of the final hybrid 5 is promising for its repeated use under heating regimes. Then, palladium loading of 5 was quantified by using inductively coupled plasma optical emission spectroscopy (ICP-OES) to be 1.5 wt%. X-ray photoelectron spectroscopy (XPS) analysis was performed to evaluate the ox-

ation state of supported palladium species onto the surface of the solid **5** (Figure 2).

Pd 3d region showed the presence of Pd^{II} species as testified by the two peaks centered at 337.5 and 342.9 eV corresponding to Pd 3d_{5/2} and Pd 3d_{3/2}, respectively.

Figure 1. TGA profiles of **3**, **4** and **5**.

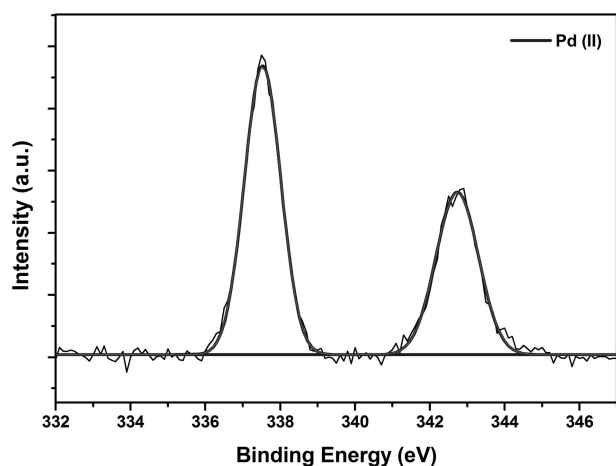


Figure 2. XPS analysis of **5**.

Small angle X-ray scattering (SAXS) measurements were carried out on both pristine and functionalized SBA-15 (Figure 3). SAXS analysis revealed the ordered mesostructure of SBA-15 showing a scattering pattern composed of a peak centered at 0.43° 2θ and two peaks, not clearly resolved, at 0.71° 2θ and 0.73° 2θ. The diffraction patterns are in line with the typical profile for hexagonal (p6mm)⁴⁹ mesoporous silica SBA-15. The most intense peak was indexed as (100) reflection, the other two features, almost merging in a broad one, were ascribed to (110) and (200) secondary peaks. According to the Bragg's law, the plane distance d (100) was computed as d = 20.55 nm and the unit cell parameter as α₀ = 23.76 nm. Moreover, the patterns of POSS modified SBA-15 **3** and **4** proved that the ordered structure of pristine SBA-15 is preserved. Indeed, the pore-to-pore distance α₀ is the same for all the solids. By comparison with pristine SBA-15, in the case of functionalized material it is possible to observe a decrease in intensity of the signals due to the presence of POSS nanostructures. However, the structural order of the pores of the pristine solid support was not significantly affected, being almost constant the ratio between the relative reflections of SBA-15, samples **3** and **4**.

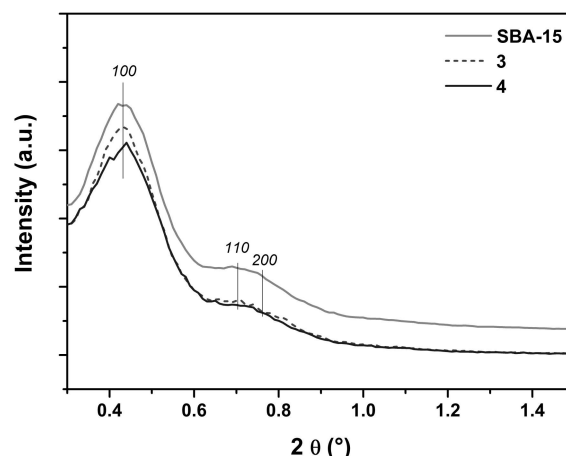
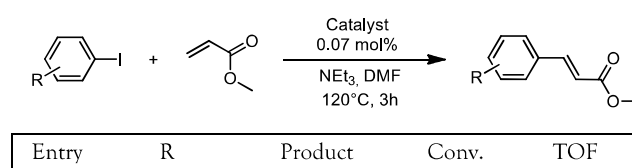
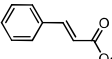


Figure 3. SAXS patterns of SBA-15, **3**, **4**.

¹³C and ²⁹Si solid state cross polarization-magic angle spinning (CP-MAS) NMR measurements were performed on both the final material **5** and its precursor **4** (Figures S1, S2). All the solid state ¹³C CP-MAS NMR experiments were recorded using the TOSS (total suppression side band) pulse sequence to displace the spinning side bands while leaving the isotropic signals. By comparison of **4** and **5** NMR spectra, it is interesting to note an excellent overlapping of the signals proving that the subsequent immobilization of palladium species had no remarkable effect on the chemical shift. In CP-MAS ¹³C NMR spectra the peculiar signals of the carbon atoms of imidazolium ring were detected in the range δ = 122-137 ppm, whereas the aliphatic ones resonated in the range δ = 10-52 ppm. The weak signal located at δ = 165 ppm can be ascribed to the C2 imidazolidinium carbon atom. In CP-MAS ²⁹Si NMR spectra the presence of Q⁴[(SiO)₄Si] (δ = -118 ppm) and Q³[(SiO)₃SiOH] (δ = -110 ppm) units was observed. The signal at δ = -75 ppm was assigned to the completely condensed T³ silicon units [R-Si(OSi)₃] of both POSS nanocage and the organosilane silicon acting as linker between the solid support and the POSS itself, whereas the signal at δ = -67 ppm was attributed to T² [R-Si(OSi)₂OR] silicon atoms bridging bulky SBA-15 to POSS units. Then, material **5** was tested as heterogeneous pre-catalyst at 0.07 mol% Pd loading in Heck and Suzuki-Miyaura reactions. In both cases, the catalytic performances were extensively evaluated in terms of selectivity, turnover number (TON, calculated as moles of aryl halide converted/moles of Pd), turnover frequency (TOF = TON h⁻¹), and recyclability. The conversion of starting aryl halides was estimated by ¹H NMR analysis of the reaction mixture. Heck reactions were performed by coupling several aryl iodides with methyl acrylate or styrene using DMF as solvent and triethylamine as base, at 120 °C. The reactions between aryl iodides and methyl acrylate afforded from high to quantitative conversion in 3 h (Table 1, Figures S3-S9). Excellent results were also obtained in terms of regioselectivity by giving *trans* isomer as the only reaction product.

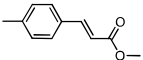
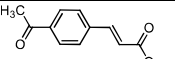
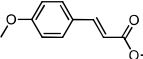
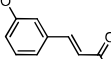
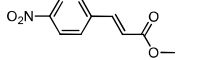
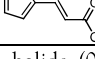
Table 1. Heck reactions catalyzed by **5**^a.



			(%)	(h ⁻¹)
1	H		>99	463

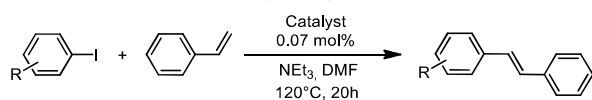
Entry	Catalyst (mol%)	Conv. (%)	TOF (h ⁻¹)
1 ^a	0.07	>99	468
2 ^b	0.007	99	4,682
3 ^c	0.0007	68	32,162

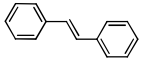
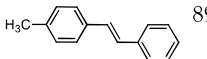
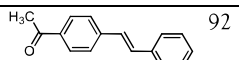
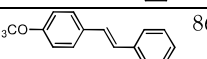
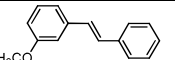
^a Reaction conditions: 4-iodoanisole (0.5 mmol), methyl acrylate (0.75 mmol), triethylamine (1 mmol), DMF (1 mL), catalyst (2.5 mg), 120 °C, 3 h; ^b Reaction conditions: 4-iodoanisole (2 mmol), methyl acrylate (3 mmol), triethylamine (4 mmol), DMF (2 mL), catalyst (1 mg), 120 °C, 3 h; ^c Reaction conditions: 4-iodoanisole (4 mmol), methyl acrylate (6 mmol), triethylamine (8 mmol), DMF (4 mL), catalyst (0.2 mg), 120 °C, 3 h.

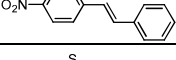
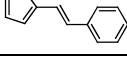
2	4-CH ₃		>99	463
3	4-COCH ₃		99	458
4	4-OCH ₃		99	458
5	3-OCH ₃		99	458
6	4-NO ₂		>99	463
7	2-C ₄ H ₃ S		91	421

^a Reaction conditions: aryl halide (0.5 mmol), methyl acrylate (0.75 mmol), triethylamine (1 mmol), DMF (1 mL), catalyst (2.5 mg), 120 °C, 3 h.

Table 2. Heck reactions catalyzed by 5^a



Entry	R	Product	S (%)	Conv. (%)	TOF (h ⁻¹)
1	H		91	99	63
2	4-CH ₃		89	98	61
3	4-COCH ₃		92	99	63
4	4-OCH ₃		86	98	59
5	3-OCH ₃		87	89	54

6	4-NO ₂		94	>99	65
7	2-C ₄ H ₃ S		95	>99	66

^aReaction conditions: aryl iodide (0.5 mmol), styrene (0.75 mmol), triethylamine (1 mmol), DMF (1 mL), catalyst (2.5 mg), 120 °C, 20 h.

However, lower levels of regioselectivity were observed in the Heck reactions between aryl iodides and styrene (Table 2, Figures S10-16). Such couplings were carried out for 20 h leading to both *trans* isomer and *gem*-alkene (5-14%). This finding, already reported in literature,⁵⁰⁻⁵¹ was ascribed to the α -migration step of the aryl group during the catalytic cycle when electron rich olefins are used. Further experiments were performed with a decreased palladium loading in the coupling between 4-iodoanisole and methyl acrylate (Table 3). Improved TOF values were achieved ranging from 468 h⁻¹ to 32,162 h⁻¹.

Table 3. Screening of catalyst loading in the reactions between 4-iodoanisole and methyl acrylate.

In order to investigate the recyclability of the material, the above mentioned coupling reaction was selected as benchmark process (Figure 4). In doing so, the solid was tested up to six cycles at 0.07 mol% without showing any decrease in the catalytic activity. Then, the catalyst recovered from the sixth cycle was successfully employed at 0.007 mol% for a seventh cycle. Interestingly, in the 7th cycle conversion was very close to that observed in the first cycle with the same catalytic loading (99%, Table 3, entry 2). This result confirms the excellent activity and recyclability of material 5.

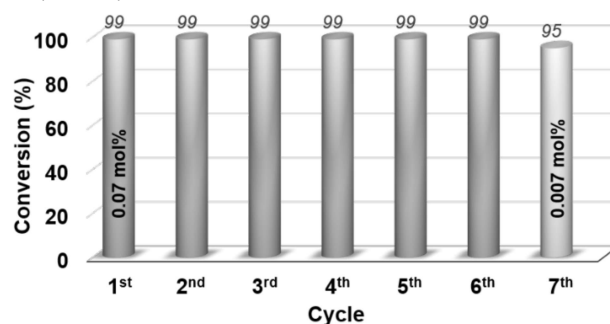


Figure 4. Recycling tests of 5 in the Heck reaction between 4-iodoanisole and methyl acrylate.

Transmission electron microscopy (TEM) measurements were carried out on both fresh and reused material (Figure 5). TEM analysis of the as-synthesized and the reused material revealed the morphology of the bidimensional mesostructured functionalized SBA-15 without showing the presence of reduced Pd nanoparticles (Figure 5).

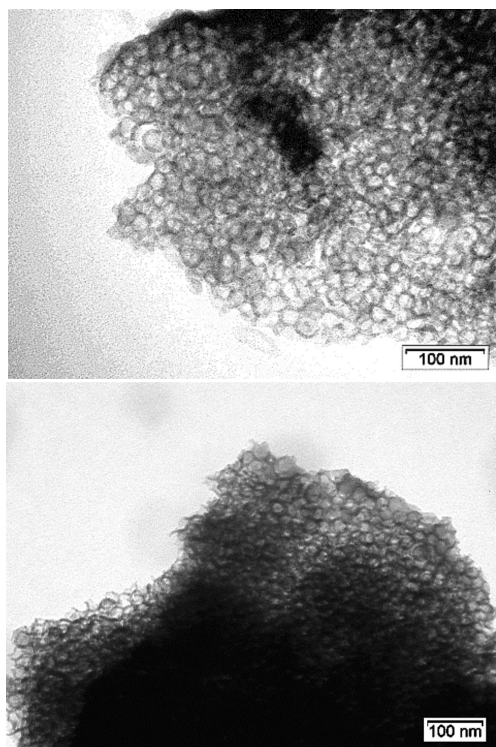


Figure 5. TEM pictures of the as-synthesized (a) and the reused catalyst 5 in the Heck reaction (b).

The reused catalyst 5 in the Heck reaction was further characterized by using XPS analyses. As evidenced by Figure 6, the XPS spectrum of the Pd 3d region clearly showed the absence of reduced Pd. Only the presence of Pd^{II} was detected.

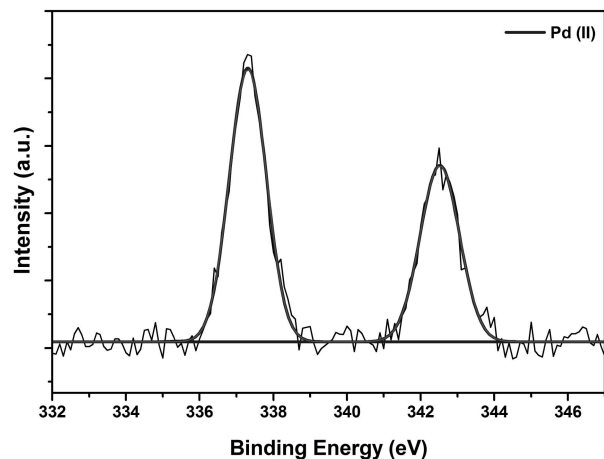


Figure 6. XPS spectrum of 5 after recycling tests in the Heck reaction.

Although the literature is plenty of supported palladium-catalyzed Heck reactions, only a few examples concern with the use of Pd^{II}-based catalysts and their study by XPS after reuse. On unmodified SiO₂, most of Pd^{II}, from Pd(acac)₂, was reduced to Pd⁰ during the Heck reaction.⁵² On the other hand, bis-carbene-pincer complexes of Pd^{II} on montmorillonite K-10 or a polystyrene-supported palladacycle did not show Pd⁰ in the XPS analysis after reuse.^{53,54} TEM analysis on reused SBA-15 metal-formin-supported Pd(II) catalyst showed the presence of Pd(0) particles. (J Porous Mater 2014, 21, 141–148)

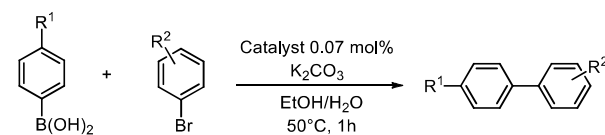
a)

We wondered if the absence of Pd(0) after reuse could be ascribed to the particular nature of the SBA-15 support. Then, we used as support for Pd species the corresponding POSS immobilized on amorphous SiO₂ that possesses a specific surface area of 250 m²/g, and a total pore volume of 0.60 cm³/g, and pore size distribution around 4.6 nm. (48). Heck reactions were carried out between 4-iodoanisole and methyl acrylate under the same condition for four cycles giving quantitative yields in the first three cycles and a 96% yield in the fourth cycle. Differently from the reused catalyst 5, XPS analysis of the SiO₂-based reused catalyst showed the presence of Pd(0) (46%) and Pd(II) species (54%) (see Figure SX and SXX).

b)

Next, the catalytic activity of 5 was investigated in Suzuki reaction between phenylboronic acid and a set of aryl bromides bearing either electron-donating or electron-withdrawing groups. The catalytic tests were run at 50 °C in a mixture ethanol/water (1:1) using K₂CO₃ as base (Table 4, Figures S17-S27).

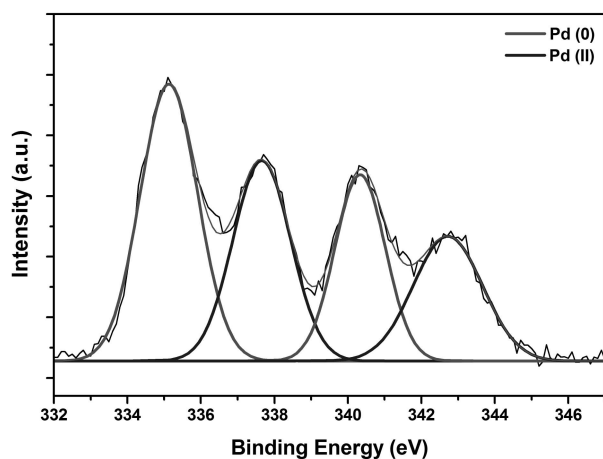
Table 4. Suzuki-Miyaura reactions catalyzed by 5^a



Entry	R ¹	R ²	Product	Conv. ^b (%)	TOF (h ⁻¹)
1	H	4-CHO		>99	1419
2	H	4-CH ₃		93	1320
3	H	3-CH ₃		99	1405
4	H	4-CN		>99	1419
5	H	4-COCH ₃		>99	1419
6	H	3-COCH ₃		>99	1419
7	H	4-NO ₂		>99	1419
8	H	4-OCH ₃		95	1348
9	H	3-OCH ₃		75	1064
10 ^c	4-CHO	4-OCH ₃		64	303
11 ^c	2-CH ₃	4-OCH ₃		88	416

^a Reaction conditions: aryl halide (0.5 mmol), phenylboronic acid (0.55 mmol), K₂CO₃ (0.6 mmol), EtOH/H₂O (1:1, 1.2 mL), catalyst (0.07 mol%), 50 °C, 1h. ^b Conversion estimated by ¹H NMR analysis. ^c Reaction performed in 3 h.

As showed in Table 4, aryl bromides with electron withdrawing substituents such as 4-CHO, 4-CN, 3-COCH₃, 4-COCH₃, and 4-NO₂ reacted with phenylboronic acid providing the corresponding cross-coupling products in quantitative conversions in 1 h. On the other hand, aryl bromides with electron-donating groups such as 3-CH₃, 4-CH₃, 3-OCH₃, 4-OCH₃, gave slightly lower conversions. Moreover, 4-bromo anisole was employed for further catalytic tests with two additional phenyl boronic acids (entries 10-11). Such reactions were performed in 3 h. The coupling between the electron-donating 4-iodoanisole and the less reactive 4-formylphenylboronic acid gave rise to a 64% conversion whereas the reaction with the *o*-tolylboronic acid led to an 88% conversion. On the ground of this finding, a screening of palladium loading was carried out in the reaction between 4-bromobenzaldehyde and phenylboronic acid (Table 5). In particular, the catalyst amount was decreased down to 0.007 and 0.0007 mol% affording turnover frequency of 13,906 and 113,515 h⁻¹, respectively. Moreover, a further catalytic test was run at higher temperature, namely 120 °C in 5 minutes with a palladium loading of 0.0007 mol%. In this case, the aryl bromide conversion was complete and led to the remarkable TOF



value of 1,685,693 h⁻¹.

Table 5. Screening of catalyst loading in the reactions between phenylboronic acid and 4-bromobenzaldehyde.

Entry	Catalyst (mol%)	Conv. (%)	TOF (h ⁻¹)
1 ^a	0.07	>99	1,405
2 ^b	0.007	99	13,906
3 ^c	0.0007	80	113,515
4 ^d	0.0007	>99	1,685,693

^a Reaction conditions: aryl bromide (0.5 mmol), phenylboronic acid (0.55 mmol), K₂CO₃ (0.6 mmol), EtOH/H₂O (1:1, 1.2 mL), catalyst (2.5 mg), 50 °C, 1 h; ^b Reaction conditions: aryl bromide (2 mmol), phenylboronic acid (2.2 mmol), K₂CO₃ (2.4 mmol), EtOH/H₂O (1:1, 2.4 mL), catalyst (1 mg), 50 °C, 1 h; ^c Reaction conditions: aryl bromide (4 mmol), phenylboronic acid (4.4 mmol), K₂CO₃ (4.8 mmol), EtOH/H₂O (1:1, 4.8 mL), catalyst (0.2 mg), 50 °C, 1 h. ^d Reaction conditions: 4-bromoacetophenone (2 mmol), phenylboronic acid (2.2 mmol), K₂CO₃ (2.4 mmol), EtOH/H₂O (1:1, 2.4 mL), catalyst (0.1 mg),

5 min, 120 °C.

Finally, the recyclability of **5** in the Suzuki reaction was verified with the coupling between 4-bromobenzaldehyde and phenylboronic acid (Figure 7).

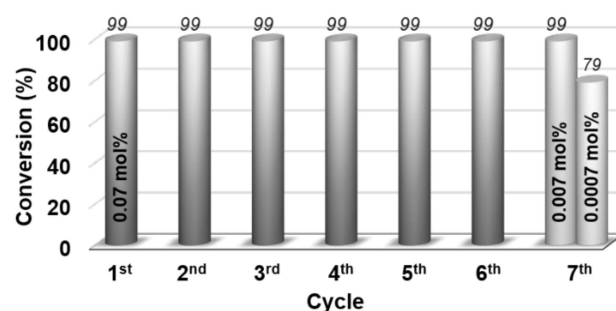


Figure 7. Recycling tests of **5** in the Suzuki reaction between 4-bromobenzaldehyde and phenylboronic acid.

It is worth to observe that 0.07 mol% of catalyst allowed to obtain a quantitative yield and conversion of the selected aryl bromide within 1 h in six consecutive runs. Next, the spent catalyst recovered from the 6th cycle was employed for two additional recycling tests with two decreased amounts of catalyst, namely 0.007 and 0.0007 mol%. By comparison with the results obtained with the as-synthesized solid **5** (Table 5, entries 2,3), it was possible to assess that the reused catalyst showed full recyclability up to seven cycles even with a decreased palladium loading. Moreover, XPS analysis of the Pd 3d core level on the spent catalyst revealed the presence of both Pd⁰ and Pd^{II} species (Figure 8). The *in situ* reduction of Pd^{II} into Pd⁰ during the catalytic tests was clearly detected by the appearance of the signals centered at 335 (3d_{3/2}) and 340.4 (3d_{5/2}) eV and resulted in a percentage of metallic Pd of 44% respect to Pd^{II}.

For the sake of comparison, as for the Heck reaction, recycling investigations were also carried out using the corresponding palladium catalyst on amorphous SiO₂. The Suzuki reaction between 4-bromobenzaldehyde and phenylboronic acid was carried for four consecutive runs giving decreasing yields from quantitative, in the first cycle, to 88% in the fourth cycle.

Figure 8. XPS spectrum of **5** after recycling tests in the Suzuki reaction.

TEM measurements were carried out on the reused material in the Suzuki reaction (Figure 9). TEM analysis of the catalyst recovered from the 6th cycle showed a fine dispersion of palladium nanoparticles. TEM pictures were collected using bright field and dark field diffraction contrast imaging. In both cases the presence of Pd NPs was clearly discernable.

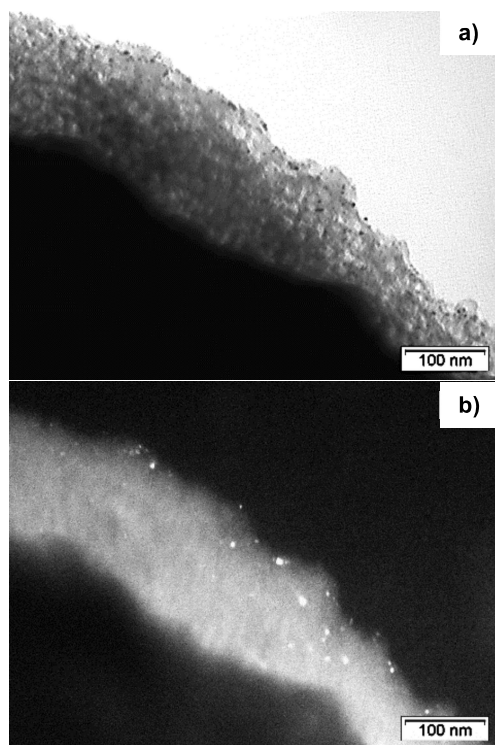


Figure 9. TEM pictures of the reused catalyst **5** in the Suzuki reaction in bright field (a) and in dark field (b).

CONCLUSIONS

Imidazolium functionalized POSS nanostructures were successfully grafted onto mesostructured SBA-15 allowing to obtain a suitable stabilizing support for Pd^{II} pre-catalytic species. Our palladium nanocomposite **5** was easily prepared *via* ionic exchange between chloride and PdCl₄²⁻ anionic species. The final hybrid was characterized by means of several techniques such as TGA, SAXS, ICP-OES, XPS and TEM. Once characterized, the catalytic activity of the material was investigated toward Suzuki and Heck cross-coupling reactions. In both processes, the catalytic performances were evaluated in terms of turnover frequency, versatility and recyclability. The versatility of **5** was investigated with a plethora of aryl halides at 0.07 mol% of Pd providing high conversions into the corresponding products. Additional tests were carried out by using the material with a palladium loading decreased to 0.0007 mol% leading to the outstanding TOF value of 1,685,693 h⁻¹ in the Suzuki reaction between 4-bromobenzaldehyde and phenylboronic acid. Moreover, the solid proved to be highly recyclable up to seven cycles without showing any decrease in the catalytic activity. The recyclability of the material was verified at 0.07 mol% of Pd for six consecutive runs. Then, the catalyst recovered from the sixth cycle was employed for further recycling experiments by using a decreased amount of Pd namely 0.007 and 0.0007 mol% for the Suzuki reaction, and 0.007 mol% in the Heck reaction. The direct comparison of the abovementioned catalytic tests with the analogous ones performed at 0.007 and 0.0007 mol% of Pd with the as-synthesized material allowed to assess the fully recyclability of the material. The comparison with the analogous catalyst in which the imidazolium functionalized POSS nanostructures were successfully grafted onto amorphous SiO₂

gave different results. In the case of Suzuki coupling reaction, the SiO₂-based imidazolium functionalized POSS-palladium catalyst was much less recyclable. In the case of Heck reaction, only a slightly decrease in yield was observed in the fourth cycle, however, the reused catalyst showed a 46% of Pd(0) by XPS analysis whereas no Pd(0) was found in the reused SBA-15-based palladium catalyst. These differences could be ascribed to the fact that the cavities of SBA-15 could act as nanoreactor for embedding Pd species in pore walls that might enhance the interaction between substrates and active Pd species. Moreover, the presence of the imidazolium POSS nanostructure within the inorganic SBA-15 could increase the stabilization of the Pd(II) species. The stabilizing role of the imidazolium POSS nanocage is evident if compared with the SBA-15-metformin-Pd(II) catalyst that, used under the same reaction conditions showed the presence of Pd(0) species. The presence of the POSS nanocage and the textural properties of SBA, can effect on the uniformly distribution of Pd species that, in turn, can help to overcome the problems of aggregation of palladium.

EXPERIMENTAL SECTION

Spectroscopic and analytical methods

Thermogravimetric analysis (TGA) measurements were carried out under oxygen flow from 100 to 1000 °C with a heating rate of 10 °C min⁻¹ in a Mettler Toledo TGA STAR Combustion chemical analysis was performed on a PerkinElmer 2400 Series II Elemental Analyzer. System.

N₂ adsorption-desorption analysis was carried out at 77 K by using a volumetric adsorption analyzer (Micromeritics Tristar 3000). Before the analysis, the sample was pretreated at 150 °C for 16 h under reduced pressure (0.1 mbar). The BET method was applied in the p/p⁰=0.05–0.30 range to calculate the specific surface area, whereas the pore size distributions were determined from the adsorption isotherm using the BJH method.

Inductively coupled plasma optical emission spectroscopy (ICP-OES) analysis was carried out with an Optima 8000 ICP-OES Spectrometer. X-ray photoelectron spectroscopy (XPS) analyses were performed with a Thermo Fisher ESCALAB 250Xi instrument equipped with a monochromatic Al K X-ray source (1486.6 eV) and a hemispherical deflector analyser (SDA) working at constant pass energy (CAE) allowing to obtain a constant energy resolution on the whole spectrum. The experiments were performed using a 200 μm diameter X-ray spot. The charge neutralization of the sample was achieved with a flood gun using low energy electrons and argon ions. The pressure in the analysis chamber was in the range of 10⁻⁸ Torr during data collection. Survey spectra were recorded with a 150 eV pass energy, whereas high-resolution individual spectra were collected with a 25 eV pass energy. Analyses of the peaks were carried out with the software Thermo Advantage, based on the non-linear squares fitting program using a weighted sum of Lorentzian and Gaussian component curves after background subtraction according to Shirley and Sherwood.⁵⁵ Full width at half maximum (FWHM) values were fixed for all the signals. Small-angle X-ray scattering (SAXS) experiments were performed on a Bruker Nanostar SAXS System equipped with 2D detector using Cu Kα radiation (λ = 1.5418 Å). The SAXS measurements were collected in the range 0.3–1.5 2θ by using a 0.02 step size and a counting time of 1.3 s per step. Solid state CP-MAS-TOSS ¹³C-NMR spectra were recorded at room temperature, on a

Bruker Avance 500 Spectrometer operating at 11.7 T, using a contact time of 2 ms, a spinning rate of 5 KHz and a Bruker probe of 4mm. CP-MAS ^{29}Si -NMR spectra were recorded at room temperature, on a Bruker Avance 500 Spectrometer operating at 11.7 T, using a contact time of 2 ms, a spinning rate of 8 KHz and a Bruker probe of 4mm. Transmission electron microscopy (TEM) pictures were recorded on a Philips TECNAI 10 microscope at 80 kV.

Synthesis of 4

Hybrid 4 was synthesized according to literature procedures.⁴⁸

Synthesis of 5

In a round bottom flask, supported imidazolium modified POSS 4 (300 mg) was dispersed and sonicated in distilled water (3 mL). In the meanwhile, a sodium tetrachloropalladate solution was prepared by using PdCl_2 (0.07 mmol, 12.4 mg), 20 equiv. of NaCl (1.4 mmol, 81.8 mg) in distilled water (4 mL). The above mixture was heated at 80°C for 20 min. Then, it was allowed to cool down to room temperature. The obtained brown Na_2PdCl_4 solution was added dropwise to the suspension of 4. The reaction mixture was stirred at room temperature for 16 h. Then, the solid was recovered by centrifugation and washed with water, methanol and diethyl ether. Before each centrifugation, the solid was sonicated for 5 min in the washing solvent. After the last washing, it was dried overnight at 60 °C obtaining catalyst 5 as pale yellow powder (299 mg).

General procedure for the Heck reaction

The catalytic tests were carried out in a 3 mL screw cap glass vial in which pre-catalyst 5 (0.07 mol%), aryl iodide (0.5 mmol), alkene (0.75 mmol), triethylamine (1 mmol) and DMF (1 mL) were placed. The reaction mixture was sonicated for a short time and heated at 120 °C under stirring for a given time. Then, the reaction mixture was allowed to cool down to room temperature, diluted with water in order to be extracted with diethyl ether. The organic layer was dried with Na_2SO_4 , filtered and evaporated under vacuum. The conversions of the products were estimated by ^1H NMR analysis.

Recycling procedure of 5 in the Heck reaction

Recycling tests were performed in a 10 mL screw cap glass vial in which pre-catalyst 5 (0.07 mol%, 10 mg), 4-iodoanisole (2 mmol), methyl acrylate (3 mmol), triethylamine (4 mmol) and DMF (4 mL) were placed. The reaction mixture was sonicated for a short time and heated at 120°C under stirring for 3h. Then, it was allowed to cool down to room temperature and centrifuged in order to recover the catalyst. The solid 5 was washed, sonicated and centrifuged with ethyl acetate, methanol and diethyl ether. Once dried, it was used for the next catalytic cycle. The recovered organic layers were evaporated under reduced pressure then treated with water and extracted with diethyl ether. The combined organic layers were dried with Na_2SO_4 , filtered and evaporated under vacuum. The conversions of the products were estimated by ^1H NMR analysis.

General procedure for the Suzuki reaction

The catalytic tests were carried out in a 3 mL screw cap glass vial in which pre-catalyst 5 (0.07 mol%), aryl bromide (0.5 mmol), phenylboronic acid (0.55 mmol) and K_2CO_3 (0.6 mmol) were placed. Then, distilled water (0.6 mL) and ethanol (0.6 mL) were added. The reaction mixture was sonicated for a short time and heated at 50 °C under stirring for a given time. Then, the reaction mixture was allowed to cool down to room temperature, diluted with water in order to be extracted with dichloromethane. The organic layer was dried with Na_2SO_4 , filtered and evaporated under vacuum. The conversions of the products were estimated by ^1H NMR analysis.

Recycling procedure of 5 in the Suzuki reaction

Recycling tests were performed in a 10 mL screw cap glass vial in which pre-catalyst 5 (0.07 mol%, 10 mg), 4-bromobenzaldehyde (2 mmol), phenylboronic acid (2.2 mmol) and K_2CO_3 (2.4 mmol) were placed. Then, distilled water (2.4 mL) and ethanol (2.4 mL) were added. The reaction mixture was sonicated for a short time and heated at 50 °C under stirring for 1h. Then, it was allowed to cool down to room temperature and centrifuged in order to recover the catalyst. The solid 5 was washed, sonicated and centrifuged with ethyl acetate, methanol and diethyl ether. Once dried, it was used for the next catalytic cycle. The recovered organic layers were evaporated under reduced pressure then treated with water and extracted with dichloromethane. The combined organic layers were dried with Na_2SO_4 , filtered and evaporated under vacuum. The conversions of the products were estimated by ^1H NMR analysis.

ASSOCIATED CONTENT

AUTHOR INFORMATION

Corresponding Author

* (Word Style "FA_Corresponding_Author_Footnote"). Give contact information for the author(s) to whom correspondence should be addressed.

Present Addresses

†If an author's address is different than the one given in the affiliation line, this information may be included here.

Funding Sources

Any funds used to support the research of the manuscript should be placed here (per journal style).

ACKNOWLEDGMENT

REFERENCES

- (1) Seechurn, C. C. C. J.; Kitching, M. O.; Colacot, T. J.; Snieckus, V. *Angewandte Chemie International Edition* **2012**, *51*, 5062-5085.
- (2) Roy, D.; Uozumi, Y. *Advanced Synthesis & Catalysis* **2018**, *360*, 602-625.
- (3) Molnár, Á. *Chemical Reviews* **2011**, *111*, 2251-2320.

- (4) Suzuki, A. *Angewandte Chemie International Edition* **2011**, *50*, 6722-6737.
- (5) Negishi, E. i. *Angewandte Chemie International Edition* **2011**, *50*, 6738-6764.
- (6) Yin; Liebscher, J. *Chemical Reviews* **2007**, *107*, 133-173.
- (7) Lamblin, M.; Nassar Hardy, L.; Hierso, J. C.; Fouquet, E.; François Xavier, F. *Advanced Synthesis & Catalysis* **2010**, *352*, 33-79.
- (8) Nicolas, O.; François Xavier, F. *ChemCatChem* **2016**, *8*, 1998-2009.
- (9) E., G. C.; Kapa, P. *Advanced Synthesis & Catalysis* **2004**, *346*, 889-900.
- (10) Sarkar, S. M.; Rahman, M. L.; Yusoff, M. M. *New Journal of Chemistry* **2015**, *39*, 3564-3570.
- (11) Opanasenko, M.; Stepnicka, P.; Cejka, J. *RSC Advances* **2014**, *4*, 65137-65162.
- (12) Pavia, C.; Ballerini, E.; Bivona, L. A.; Giacalone, F.; Aprile, C.; Vaccaro, L.; Gruttadauria, M. *Advanced Synthesis & Catalysis* **2013**, *355*, 2007-2018.
- (13) Kumbhar, A. *Topics in Current Chemistry* **2016**, *375*, 2.
- (14) Wang, C. A.; Li, Y. W.; Hou, X. M.; Han, Y. F.; Nie, K.; Zhang, J. P. *ChemistrySelect* **2016**, *1*, 1371-1376.
- (15) Wang, X.; Min, S.; Das, S. K.; Fan, W.; Huang, K.-W.; Lai, Z. *Journal of Catalysis* **2017**, *355*, 101-109.
- (16) Navalón, S.; Álvaro, M.; García, H. *ChemCatChem* **2013**, *5*, 3460-3480.
- (17) Ma, R.; Yang, P.; Bian, F. *New Journal of Chemistry* **2018**, *42*, 4748-4756.
- (18) Manjunatha, K.; Koley, T. S.; Kandathil, V.; Dateer, R. B.; Balakrishna, G.; Sasidhar, B. S.; Patil, S. A.; Patil, S. A. *Applied Organometallic Chemistry* **2018**, *32*, e4266.
- (19) Adib, M.; Karimi-Nami, R.; Veisi, H. *New Journal of Chemistry* **2016**, *40*, 4945-4951.
- (20) Giacalone, F.; Campisciano, V.; Calabrese, C.; La Parola, V.; Syrgiannis, Z.; Prato, M.; Gruttadauria, M. *ACS Nano* **2016**, *10*, 4627-4636.
- (21) Barahman, M.; S., P. F.; Mozghan, N. *Applied Organometallic Chemistry* **2015**, *29*, 40-44.
- (22) Navidi, M.; Rezaei, N.; Movassagh, B. *Journal of Organometallic Chemistry* **2013**, *743*, 63-69.
- (23) Campisciano, V.; Parola, V. L.; F.Liotta, L.; Giacalone, F.; Gruttadauria, M. *Chemistry – A European Journal* **2015**, *21*, 3327-3334.
- (24) Massaro, M.; Riela, S.; Lazzara, G.; Gruttadauria, M.; Milioto, S.; Noto, R. *Applied Organometallic Chemistry* **2014**, *28*, 234-238.
- (25) Massaro, M.; Schembri, V.; Campisciano, V.; Cavallaro, G.; Lazzara, G.; Milioto, S.; Noto, R.; Parisi, F.; Riela, S. *RSC Advances* **2016**, *6*, 55312-55318.
- (26) Rong, S.; Bing, L.; Bo Geng, L.; Suyun, J. *ChemCatChem* **2016**, *8*, 3261-3271.
- (27) Li, X.; Van Zeeland, R.; Maligal-Ganesh, R. V.; Pei, Y.; Power, G.; Stanley, L.; Huang, W. *ACS Catalysis* **2016**, *6*, 6324-6328.
- (28) Xiong, G.; Chen, X.-L.; You, L.-X.; Ren, B.-Y.; Ding, F.; Dragutan, I.; Dragutan, V.; Sun, Y.-G. *Journal of Catalysis* **2018**, *361*, 116-125.
- (29) Neouze, M.-A. *Journal of Materials Chemistry* **2010**, *20*, 9593-9607.
- (30) Serpell, C. J.; Cookson, J.; Thompson, A. L.; Brown, C. M.; Beer, P. D. *Dalton Transactions* **2013**, *42*, 1385-1393.
- (31) Silarska, E.; Trzeciak, A. M.; Pernak, J.; Skrzypczak, A. *Applied Catalysis A: General* **2013**, *466*, 216-223.
- (32) Song, H.; Yan, N.; Fei, Z.; Kilpin, K. J.; Scopelliti, R.; Li, X.; Dyson, P. J. *Catalysis Today* **2012**, *183*, 172-177.
- (33) Zawartka, W.; Gniewek, A.; Trzeciak, A. M.; Zió kowski, J. J.; Pernak, J. *Journal of Molecular Catalysis A: Chemical* **2009**, *304*, 8-15.
- (34) Daisy, M. M.; Parul, G. *Applied Organometallic Chemistry* **2016**, *30*, 759-766.
- (35) Veerakumar, P.; Thanasekaran, P.; Lu, K.-L.; Liu, S.-B.; Rajagopal, S. *ACS Sustainable Chemistry & Engineering* **2017**, *5*, 6357-6376.
- (36) Polshettiwar, V.; Len, C.; Fihri, A. *Coordination Chemistry Reviews* **2009**, *253*, 2599-2626.
- (37) Giacalone, F.; Campisciano, V.; Calabrese, C.; La Parola, V.; Liotta, L. F.; Aprile, C.; Gruttadauria, M. *Journal of Materials Chemistry A* **2016**, *4*, 17193-17206.
- (38) Bivona, L. A.; Giacalone, F.; Carbonell, E.; Gruttadauria, M.; Aprile, C. *ChemCatChem* **2016**, *8*, 1685-1691.
- (39) Mohapatra, S.; Chairprasert, T.; Sodkhomkhum, R.; Kunthom, R.; Hanpravit, S.; Sangtrirutnugul, P.; Ervithayasuporn, V. *ChemistrySelect* **2016**, *1*, 5353-5357.
- (40) Somjit, V.; Man, M. W. C.; Ouali, A.; Sangtrirutnugul, P.; Ervithayasuporn, V. *ChemistrySelect* **2018**, *3*, 753-759.
- (41) Cordes, D. B.; Lickiss, P. D.; Rataboul, F. *Chemical Reviews* **2010**, *110*, 2081-2173.
- (42) Li, Y.; Dong, X.-H.; Zou, Y.; Wang, Z.; Yue, K.; Huang, M.; Liu, H.; Feng, X.; Lin, Z.; Zhang, W.; Zhang, W.-B.; Cheng, S. Z. D. *Polymer* **2017**, *125*, 303-329.
- (43) Li, Z.; Kong, J.; Wang, F.; He, C. *Journal of Materials Chemistry C* **2017**, *5*, 5283-5298.
- (44) Zhou, H.; Ye, Q.; Xu, J. *Materials Chemistry Frontiers* **2017**, *1*, 212-230.
- (45) Ghanbari, H.; Cousins, B. G.; Seifalian, A. M. *Macromolecular Rapid Communications* **2011**, *32*, 1032-1046.
- (46) Zhu, Y.-X.; Jia, H.-R.; Pan, G.-Y.; Ulrich, N. W.; Chen, Z.; Wu, F.-G. *Journal of the American Chemical Society* **2018**, *140*, 4062-4070.
- (47) Kaneko, Y. *Polymer* **2018**, *144*, 205-224.
- (48) Calabrese, C.; Liotta, L. F.; Giacalone, F.; Gruttadauria, M.; Aprile, C. *ChemCatChem*.
- (49) Zhao, D.; Feng, J.; Huo, Q.; Melosh, N.; Fredrickson, G. H.; Chmelka, B. F.; Stucky, G. D. *Science* **1998**, *279*, 548-552.
- (50) Fristrup, P.; Le Quement, S.; Tanner, D.; Norrby, P.-O. *Organometallics* **2004**, *23*, 6160-6165.
- (51) Ruan, J.; Xiao, J. *Accounts of Chemical Research* **2011**, *44*, 614-626.

(52) Huang, L.; Wang, Y.; Wang, Z.; Chen, F.; Tan, J.; Wong, P. K. *Physical Chemistry* **2012**, *2*, 27-34.

(53) Poyatos, M.; Márquez, F.; Peris, E.; Claver, C.; Fernandez, E. *New Journal of Chemistry* **2003**, *27*, 425-431.

(54) Alacid, E.; Nájera, C. *ARKIVOC* **2008**, *8*, 50-67.

(55) Shirley, D. A. *Physical Review B* **1972**, *5*, 4709-4714.